Sensors and Materials, Vol. 32, No. 4 (2020) 1381–1387
MYU Tokyo

S & M 2184

Radiation-induced Luminescence Properties of $SrBr_2$ Transparent Ceramics Doped with Different Eu Concentrations

Hiromi Kimura,* Takumi Kato, Daisuke Nakauchi,
Noriaki Kawaguchi, and Takayuki Yanagida

Division of Materials Science, Nara Institute of Science and Technology (NAIST),
8916-5 Takayama-cho, Ikoma-shi, Nara 630-0192, Japan

(Received December 21, 2019; accepted March 10, 2020)

Keywords: transparent ceramics, scintillation, photoluminescence, $SrBr_2$

We successfully developed Eu-doped $SrBr_2$ transparent ceramics with different Eu concentrations by spark plasma sintering and evaluated their optical and scintillation properties. As optical properties, the diffuse transmittance of the 0.01% Eu-doped sample was ~60% in the visible range. All the samples showed two absorption bands at around 250 and 350 nm, the origin of which was the 4f–5d (e_g, t_{2g}) transitions of Eu^{2+}. Regarding scintillation spectra, the spectral shapes of all the Eu-doped $SrBr_2$ transparent ceramics were similar to that of single crystals. In pulse height spectra, the photoabsorption peak of the 0.01 and 0.1% Eu-doped samples was confirmed, and the estimated light yields were 6600 and 13300 photons/MeV, respectively. Regarding afterglow properties, the afterglow levels of the 0.01 and 0.1% Eu-doped samples were comparable to that of a conventional Tl-doped CsI scintillator.

1. Introduction

Scintillation detectors have been used for various fields such as medicine,[1–3] security,[4] detection of hidden special nuclear materials in well logging,[5] and astrophysics.[6] Such detectors consisted of scintillators and photodetectors, such as a photomultiplier tube (PMT) and a Si photodiode. Scintillators absorb the energy of ionizing radiation (e.g., X- and γ-rays) and then rapidly convert it to many low-energy photons immediately. In general, the required scintillation properties for X- and γ-ray detection are high light yield, short lifetime, high effective atomic number, and low afterglow.[7] However, scintillators that completely satisfy the above requirements have not been found; therefore, the development of scintillators has been performed continuously.

The recent trend in the development of scintillators is their design using a combination of an inorganic material as a host matrix and rare-earth ions as emission centers.[8–13] The host matrix effectively absorbs ionizing radiation, and then the emission centers convert the absorbed energy to visible photons. In the 2000s, Ce-doped $Gd_3Al_2Ga_3O_{12}$ (GAGG) and Eu-

*Corresponding author: e-mail: kimura.hiromi.kf1@ms.naist.jp
https://doi.org/10.18494/SAM.2020.2750

ISSN 0914-4935 © MYU K.K.

doped SrI_2 single crystals were reported and commercialized because they showed high light yields (*LY*s) of ~46000 and ~82000 photons/MeV and acceptable lifetimes of ~50 ns and ~4 μs, respectively.[14,15]

Thus far, most practical scintillators have been used in the form of bulk single crystals because single crystals have high optical qualities. In recent years, garnet-type oxides in the form of transparent ceramics have been developed, and some transparent ceramics, such as Ce-doped GAGG[14] and Ce-doped $Y_3Al_5O_{12}$,[16] exhibited higher *LY*s than single crystals. Additionally, transparent ceramics have many advantages, such as high mechanical strength and flexible shape, in comparison with single crystals. However, most studies have been on oxide materials; thus, we have started to investigate bromide materials in the form of transparent ceramics in terms of their scintillation properties.[17–19]

In this paper, we focus on Eu-doped $SrBr_2$ in the form of transparent ceramics. As indicated in past reports, Eu-doped $SrBr_2$ single crystals show a primary emission peak at around 410 nm in scintillation spectra, and their emission wavelength is suitable for the sensitivity of PMT.[20] In addition, the *LY* and energy resolution were 20000 photons/MeV and 7% at 662 keV, respectively.[21] However, there are no reports on the scintillation properties of Eu-doped $SrBr_2$ transparent ceramics. Therefore, we developed Eu-doped $SrBr_2$ transparent ceramics with different Eu concentrations (0.01, 0.1, and 1 mol%) by spark plasma sintering (SPS) and examined their optical and scintillation properties.

2. Experimental Methods

$SrBr_2$ transparent ceramics doped with various Eu concentrations (0.01, 0.1, and 1 mol%) were synthesized by SPS. As the starting powders, $SrBr_2 \cdot 6H_2O$ (≥99%, Mitsuwa's Pure Chemicals) and $EuCl_3 \cdot 6H_2O$ (≥99.9%, Furutachi Chemical) were used. The solubility of $SrBr_2$ was 107 g/100 g in water at 20 °C, which is lower than that of SrI_2 scintillators.[22] The powders of 0.01, 0.1, and 1% Eu-doped $SrBr_2$ were mixed using a mortar and pestle, and then the mixed powder was dried by heating at ~250 °C for 1 h in vacuum. The dried powder was introduced into a cylindrical graphite die and held between two graphite punches. The inner parts of the graphite die and punch were covered with graphite sheets. The sintering conditions are as follows. The temperature was increased up to 150 °C at a rate of 50 °C/min and maintained for 5 min. Then, it was further increased at a rate of 10 °C/min to 450 °C and maintained for 20 min while applying a pressure of 100 MPa in vacuum. The surfaces of the samples were mechanically polished with sandpaper (3000 grits). The prepared samples were evaluated as described below.

Optical properties were evaluated on the basis of the diffuse transmittance spectra measured using a spectrophotometer (SolidSpec-3700, Shimadzu) in the spectral range of 200 to 800 nm. The photoluminescence (PL) excitation and emission contour graph and quantum yields (*QY*s) were evaluated using a Quantaurus-QY (C11347, Hamamatsu Photonics). PL lifetimes were analyzed on the basis of the PL decay curves measured using a Quantaurus-τ (C11367, Hamamatsu Photonics). Scintillation properties were evaluated on the basis of the X-ray-induced scintillation spectra obtained using our original setup described previously.[14] The

operated bias voltage and tube current of the X-ray generator were 40 kV and 1.2 mA, respectively. The scintillation decay and afterglow curves were measured using an X-ray-induced afterglow characterization system.[23] To evaluate the *LY*s, we measured the pulse height spectra using a laboratory-built setup, which is described elsewhere in detail.[17]

3. Results and Discussion

Figure 1 shows a photograph of the synthesized Eu-doped $SrBr_2$ transparent ceramics. The thickness of all the samples was fixed at approximately 1.0 mm. The mash patterns on the back of samples were seen though the samples. The diffuse transmittance spectra of Eu-doped $SrBr_2$ transparent ceramics are shown in Fig. 2. The transmittance of the synthesized samples decreased with increasing Eu concentrations, and the color of the 1% Eu-doped sample was slightly grey. As possible reasons, the color of the 1% Eu-doped sample may be due to the contamination of carbon from the graphite assembly or the generation of some defects by Eu doping. All the samples showed absorption bands at around 250 and 350 nm, the origin of which was the 4f–5d (e_g, t_{2g}) transitions of Eu^{2+}.[24]

Figure 3 shows the PL excitation and emission contour graphs of Eu-doped $SrBr_2$ transparent ceramics. All the samples showed an emission peak at around 410 nm under excitation at around 350 nm, and the excitation spectra were similar to the absorption spectra. The spectral features were consistent with past reports on Eu-doped $SrBr_2$ single crystals,[20] the origin of which would be the 5d–4f transitions of Eu^{2+}. The PL decay curves of Eu-doped $SrBr_2$ transparent ceramics are shown in Fig. 4. The monitored emission and excitation wavelengths were 410 and 280 nm, respectively. The decay curves were approximated by a single exponential decay function, and the lifetimes of all the samples were 0.41–0.47 μs. These values were typical for the 5d–4f transitions of Eu^{2+}.[25] The *QY*s of 0.01, 0.1, and 1% Eu-doped $SrBr_2$ transparent ceramics were 50.5, 38.6, and 14.7%, respectively.

Figure 5 shows the X-ray-induced scintillation spectra of Eu-doped $SrBr_2$ transparent ceramics. In all the samples, the spectrum consisted of two peaks at around 410 and 500 nm. The spectral shapes were consistent with previous reports on Eu-doped $SrBr_2$ single crystals.[20]

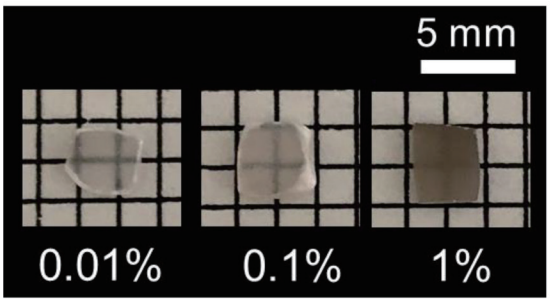

Fig. 1. (Color online) Synthesized 0.01, 0.1, and 1% Eu-doped $SrBr_2$ transparent ceramics.

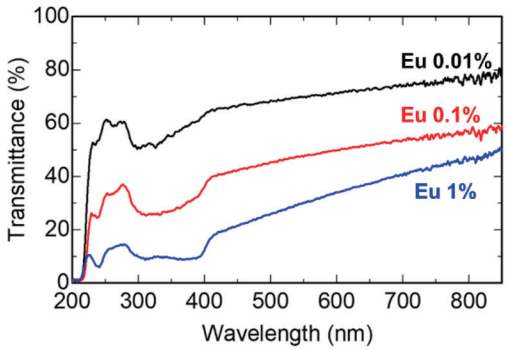

Fig. 2. (Color online) Diffuse transmittance spectra of 0.01, 0.1, and 1% Eu-doped $SrBr_2$ transparent ceramics.

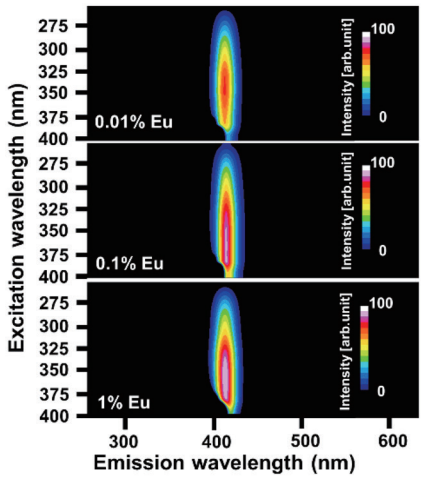

Fig. 3. (Color online) PL excitation and emission contour graphs of 0.01, 0.1, and 1% Eu-doped $SrBr_2$ transparent ceramics.

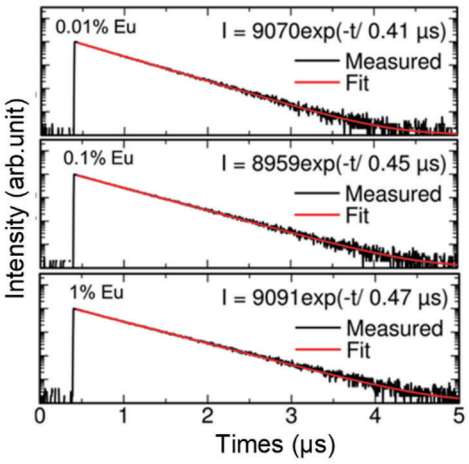

Fig. 4. (Color online) PL decay curves of 0.01, 0.1, and 1% Eu-doped $SrBr_2$ transparent ceramics monitored at 410 nm under 280 nm excitation.

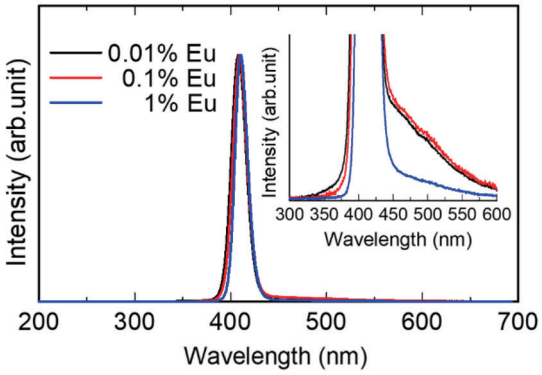

Fig. 5. (Color online) X-ray-induced scintillation spectra of Eu-doped $SrBr_2$ transparent ceramics. The inset shows an expansion of the 300–660 nm region.

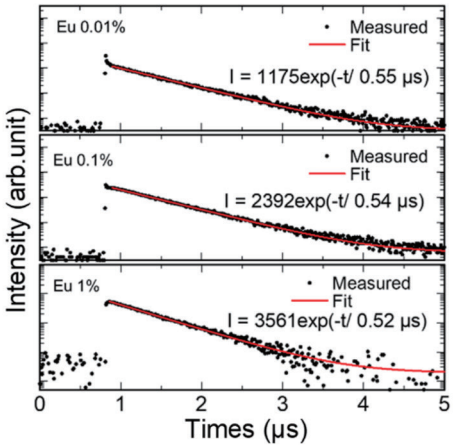

Fig. 6. (Color online) X-ray-induced scintillation decay curves of Eu-doped $SrBr_2$ transparent ceramics.

The emission peaks at around 410 and 500 nm were due to the 5d–4f transitions of Eu^{2+}[20] and the F–VK center recombinations,[26] respectively. The X-ray-induced scintillation decay curves of Eu-doped $SrBr_2$ transparent ceramics are shown in Fig. 6. The decay curves were well approximated by a single exponential decay function. The lifetimes were 0.52–0.55 μs, typical of the 5d–4f transitions of Eu^{2+}.[25] The lifetimes due to emission around 500 nm was not observed because the intensity of the emission peak at around 500 nm was lower than that at around 410 nm. Figure 7 shows the pulse height spectra of ^{137}Cs γ-rays measured using Eu-doped $SrBr_2$ transparent ceramics. To calibrate the peak channel to *LY*, we measured the pulse height spectrum of the Tl-doped NaI commercial scintillator (40000 photons/MeV).[27] In the 0.01 and 0.1%Eu-doped $SrBr_2$ transparent ceramics, the photoabsorption peak was confirmed and

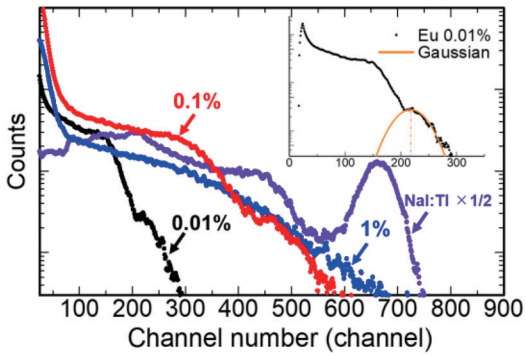

Fig. 7. (Color online) Pulse height spectra of ^{137}Cs γ-rays measured using Eu-doped $SrBr_2$ transparent ceramics and Tl-doped NaI commercial scintillators. The inset shows the experimental data (0.01% Eu) with a fitted Gaussian function.

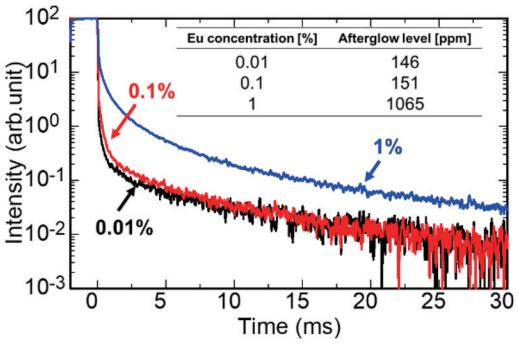

Fig. 8. (Color online) Afterglow curves of Eu-doped $SrBr_2$ transparent ceramics after 2 ms X-ray irradiation.

fitted by a Gaussian function. As a representative, the Gaussian fitting for the 0.01% Eu-doped sample is illustrated in the inset of Fig. 7. The peak positions of the 0.01 and 0.1% Eu-doped samples and the Tl-doped NaI scintillator were at 217 and 440 and 1325 channels, respectively. Here, the *QY*s of PMT were taken into consideration. The estimated *LY*s of the 0.01 and 0.1% Eu-doped samples were 6600 and 13300 photons/MeV with a typical error of ±10%. According to a previous report, the *LY* of a 0.5% Eu-doped $SrBr_2$ single crystal was 20000 photons/MeV.[21] The *LY* of Eu-doped $SrBr_2$ transparent ceramics was lower than that of Eu-doped $SrBr_2$ single crystals. As possible reasons, the ceramics generally have some defects in comparison with the single crystals, and such defects would act as quenching or trapping centers. However, when the synthesis methods and conditions are optimized to be the same as those for some transparent ceramic materials, the *LY* may be improved.

Figure 8 shows the afterglow curves of Eu-doped $SrBr_2$ transparent ceramics after 2 ms X-ray irradiation. Here, the afterglow level is defined as Afterglow level (%) = $100 \times (I_2 - I_{BG})/(I_1 - I_{BG})$, where I_{BG}, I_1, and I_2 denote the background signal, the signal intensity during X-ray irradiation, and the signal obtained 20 ms after the irradiation was cut off. The afterglow levels of the 0.01, 0.1, and 1% Eu-doped $SrBr_2$ samples were 0.0416, 0.0151, and 0.1065%, respectively. With the increasing Eu concentration, the afterglow level increased. In particular, the afterglow levels of the 0.01 and 0.1% Eu-doped samples were comparable to that of a conventional Tl-doped CsI scintillator.[23]

4. Conclusions

We have developed Eu-doped $SrBr_2$ transparent ceramics with different Eu concentrations by SPS and evaluated their optical and scintillation properties. Regarding optical properties, the 0.01% Eu-doped sample showed a high transmittance (~60%), and the absorption bands at around 250 and 350 nm were observed. The *QY*s of the 0.01, 0.1, and 1% Eu-doped samples were 50.5, 38.6, and 14.7%, respectively. Regarding scintillation properties, all the samples showed two

emission peaks at around 410 and 500 nm, the origin of which was the 5d–4f transitions of Eu^{2+} and the F–VK center recombinations. The decay curves were well approximated by a single exponential decay function, and the lifetimes were 0.52–0.55 μs. The *LY*s of the 0.01 and 0.1% Eu-doped samples were 6600 and 13300 photons/MeV, respectively. The afterglow levels of the 0.01, 0.1, and 1% Eu-doped $SrBr_2$ samples were 0.0416, 0.0151, and 0.1065%, respectively, which were comparable to that of a conventional Tl-doped CsI scintillator.

Acknowledgments

This work was supported by Grants-in-Aid for Scientific Research A (17H01375), Scientific Research B (18H03468), and JSPS Research Fellow (19J22091) from JSPS. Support from the Cooperative Research Project of Research Institute of Electronics, Shizuoka University, Terumo Foundation for Life Sciences and Arts, Izumi Science and Technology Foundation, Kazuchika Okura Memorial Foundation, Iwatani Naoji Foundation, and NAIST Foundation is also acknowledged.

References

1 C. W. E. van Eijk: Nucl. Instrum. Methods Phys. Res., Sect. A **509** (2003) 17.
2 H. Nanto, A. Nishimura, M. Kuroda, Y. Takei, Y. Nakano, T. Shoji, T. Yanagita, and S. Kasai: Nucl. Instrum. Methods Phys. Res., Sect. A **580** (2007) 278.
3 N. M. Winch, A. Edgar, and C. M. Bartle: Nucl. Instrum. Methods Phys. Res., Sect. A **763** (2014) 394.
4 J. M. Hall, S. Asztalos, P. Biltoft, J. Church, M. A. Descalle, T. Luu, D. Manatt, G. Mauger, E. Norman, D. Petersen, J. Pruet, S. Prussin, and D. Slaughter: Nucl. Instrum. Methods Phys. Res., Sect. B **261** (2007) 337.
5 Y. Tsubota, J. H. Kaneko, M. Higuchi, S. Nishiyama, and H. Ishibashi: Appl. Phys. Express **8** (2015) 062602.
6 T. Itoh, T. Yanagida, M. Kokubun, M. Sato, R. Miyawaki, K. Makishima, T. Takashima, T. Tanaka, K. Nakazawa, T. Takahashi, N. Shimura, and H. Ishibashi: Nucl. Instrum. Methods Phys. Res. Sect. A **579** (2007) 239.
7 T. Yanagida: Proc. Japan Acad. Ser. B **94** (2018) 75.
8 H. Kimura, F. Nakamura, T. Kato, D. Nakauchi, G. Okada, N. Kawaguchi, and T. Yanagida: Sens. Mater. **30** (2018) 1555.
9 G. Okada, M. Akatsuka, H. Kimura, M. Mori, N. Kawano, N. Kawaguchi, and T. Yanagida: Sens. Mater. **30** (2018) 1547.
10 N. Kawaguchi, H. Kimura, M. Akatsuka, G. Okada, N. Kawano, K. Fukuda, and T. Yanagida: Sens. Mater. **30** (2018) 1585.
11 D. Nakauchi, N. Kawaguchi, and T. Yanagida: Sens. Mater. **31** (2019) 1249.
12 H. Fukushima, D. Nakauchi, N. Kawaguchi, and T. Yanagida: Sens. Mater. **31** (2019) 1273.
13 D. Nakauchi, F. Nakamura, G. Okada, H. Kimura, N. Kawaguchi, and T. Yanagida: Radiat. Meas. **126** (2019) 106127.
14 T. Yanagida, K. Kamada, Y. Fujimoto, H. Yagi, and T. Yanagitani: Opt. Mater. **35** (2013) 2480.
15 T. Yanagida, M. Koshimizu, G. Okada, T. Kojima, J. Osada, and N. Kawaguchi: Opt. Mater. **61** (2016) 119.
16 T. Yanagida, T. Itoh, H. Takahashi, S. Hirakuri, M. Kokubun, K. Makishima, M. Sato, T. Enoto, T. Yanagitani, H. Yagi, T. Shigetad, and T. Ito: Nucl. Instrum. Methods Phys. Res., Sect. A **579** (2007) 23.
17 H. Kimura, F. Nakamura, T. Kato, D. Nakauchi, G. Okada, N. Kawaguchi, and T. Yanagida: J. Mater. Sci. Mater. Electron. **29** (2018) 8498.
18 H. Kimura, T. Kato, D. Nakauchi, N. Kawaguchi, and T. Yanagida: J. Mater. Sci. Mater. Electron. **30** (2019) 16755.
19 H. Kimura, F. Nakamura, T. Kato, D. Nakauchi, N. Kawano, G. Okada, N. Kawaguchi, and T. Yanagida: J. Ceram. Soc. Jpn. **126** (2018) 184.
20 D. H. Gahane, N. S. Kokode, P. L. Muthal, S. M. Dhopte, and S. V. Moharil: J. Alloys Compd. **484** (2009) 660.

21 N. J. Cherepy, S. A. Payne, S. J. Asztalos, G. Hull, J. D. Kuntz, T. Niedermayr, S. Pimputkar, J. J. Roberts, R. D. Sanner, T. M. Tillotson, E. van Loef, C. M. Wilson, K. S. Shah, U. N. Roy, R. Hawrami, A. Burger, L. A. Boatner, W.-S. Choong, and W. W. Moses: IEEE Trans. Nucl. Sci. **56** (2009) 873.
22 W. M. Haynes: CRC Handbook of Chemistry and Physics, 96th Edition (CRC Press, Boca Raton, 2015).
23 T. Yanagida, Y. Fujimoto, T. Ito, K. Uchiyama, and K. Mori: Appl. Phys. Express **7** (2014) 062401.
24 J. Hernandez A., W. K. Cory, and J. Rubio O.: J. Chem. Phys. **72** (1980) 198.
25 H. Kimura, F. Nakamura, T. Kato, D. Nakauchi, N. Kawano, G. Okada, N. Kawaguchi, and T. Yanagida: Optik **157** (2018) 421.
26 M. Secu, S. Schweizer, U. Rogulis, and J.-M. Spaeth: J. Phys. Condens. Matter. **15** (2003) 2061.
27 D. Engelkemeir: Rev. Sci. Instrum. **27** (1956) 589.